Artificial Allosteric System. 2. Cooperative 1-Methylimidazole Binding to an Artificial Allosteric System, Zinc-Gable Porphyrin-Dipyridylmethane Complex

Iwao Tabushi,* Shin-ichi Kugimiya, Michael G. Kinnaird,† and Tomikazu Sasaki

Contribution from the Department of Synthetic Chemistry, Kyoto University, Sakyo-ku, Kyoto 606, Japan. *Received July 23, 1984*

Abstract: Base binding to a series of monometal or bismetal complexes (Zn and Fe) of gable porphyrin was investigated by the use of NMR and electronic spectroscopy. *N,N'*-Diimidazolylmethane and γ,γ'-dipyridylmethane (DPM) were used as rigid dimeric bridging ligands, and 1-methylimidazole and γ-picoline were used as monomeric ligands. Dimeric (bridging) ligands bind to monometal-gable complexes in noncooperative fashion and mainly from the exo side. For bismetal-gable complexes DPM binds from the endo side much more strongly than monomeric ligands. The second binding of the DPM to bismetal-gable was very much enhanced compared to the first binding. This leads to formation of stable allosteric systems, gable·M^{II}·bridging ligand complexes. Due to the remarkably enhanced stability of the "bridged" structure, the pentacoodinate complex M^{II}_2·gable was formed nearly quantitatively even for the Fe^{II} species at low ligand concentration, in an interesting contrast to normal porphyrin·Fe^{II} complexes. The binding of 1-methylimidazole to the allosteric system thus formed, gable porphyrin·Zn_2·DPM bridged complex, showed remarkable allosteric behavior with a maximal Hill coefficient of 1.7 at 1.56×10^{-4} M of DPM. The magnitude of the Hill coefficient was dependent on the bridging ligand concentration. This allosteric binding of 1-methylimidazole is interpreted in terms of the (i) original T structure, (ii) first unfavorable base binding, (iii) structure change, T → R, induced by the first base binding, (iv) cleavage of intersubunit linking, transfering structure change, T → R, to the second site, and (v) favorable second base binding.

The biological allosteric effect[1] is now reasonably well understood although the study has been limited to examples like cooperative O_2 of CO binding to hemoglobin.[2] The simplest mechanistic interpretation of the cooperative O_2 binding to native hemoglobin is shown in Chart I or Scheme I in a somewhat generalized fashion. As shown in Chart I, allosteric binding is a sequence of chemical events. Total modelling has not yet been successful but partial modelling is reported recently by the use of entirely artificial systems—on conformation change,[3] on induced indirect structure change connecting with intersubunit bond cleavage (for O_2 binding),[4] or on subunit association (for base binding).[5] Thus, the new concept of an *artificial allosteric system* is becoming recognized.[4-7] However, the limited number of examples available at present prevents a detailed discussion about the general nature of allosterism. Addition of more information is necessary and important to clarify the nature of every chemical event partially participating in total allosterism.

The authors now wish to report that the gable porphyrin-biszinc-dipyridylmethane (or diimidazolylmethane) complex is predominantly formed in the bridged T structure, showing remarkable cooperativity in the binding of 1-methylimidazole, where the first base binding strongly enhances the second base binding. This enhancement is ascribed to the local structure change (T → R) at the second free site induced by the intersubunit bond cleavage, which is induced by the base binding at the first site.

Results and Discussions

Preparation of Gable Porphyrin and Its Metal Complexes. Preparation of *m*-bis(*meso*-triphenylporphyrinyl)benzene (gable porphyrin) (**1**) was carried out via the stepwise porphyrin ring closure as reported elsewhere.[5b] Monometal and bismetal complexes of gable porphyrin **2** are prepared according to the usual metalation procedures.[8,9] Monometalation proceeds smoothly, giving a mixture of bismetal, monometal, and free porphyrins in a nearly statistical ratio (e.g., gable·Zn_2:gable·Zn_1:gable, 30%:41%:20%). The monometal porphyrin was easily separated and purified from other products by chromatography on Al_2O_3 (CH_2Cl_2/hexane (2:1) followed by recrystallization.

The structures of the gable porphyrin and metal-gable porphyrins were determined by ^{13}C NMR, ^1H NMR, electronic spectra, mass spectra, and elemental analysis as described in the Experimental Section. The ^1H NMR spectra of the gable and

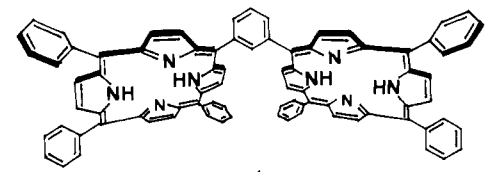

1

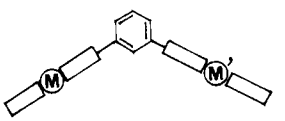

M	M'	
Co	Co	(8a)
Zn	H_2	(8b)
Zn	Zn	(8c)
Fe^{3+}	Fe^{3+}	(8d)
Fe^{2+}	Fe^{2+}	(8e)

metal-gable porphyrins, especially the latter, showed sharp absorptions (see Figure 1), strongly suggesting that porphyrin planes retain their freedom of internal (restricted) rotation in the dimers.[10] The visible spectra of the free base and some of the metal-gable

† Responsible only for NMR study of base binding.

(1) (a) Monod, J.; Changeux, J. P.; Jacob, F. *J. Mol. Biol.* **1963**, *6*, 306-329. (b) Monod, J.; Wyman, J.; Changeux, J. P. *Ibid.* **1965**, *12*, 88-118. (c) Koshland, D. E.; Nemethy, G.; Filmer, D. *Biochemistry* **1966**, *5*, 365-385.

(2) Perutz, M. F. *Annu. Rev. Biochem.* **1979**, *48*, 327-386.

(3) (a) Rebek, J., Jr.; Costello, T.; Marshall, L. *J. Am. Chem. Soc.* **1983**, *105*, 6759-6760. (b) Rebek, J., Jr. *Acc. Chem. Res.* **1984**, *17*, 258-264.

(4) Traylor, T. G.; Mitchell, M. J.; Ciccone, J. P.; Nelson, S. *J. Am. Chem. Soc.* **1982**, *104*, 4986-4989.

(5) (a) Tabushi, I.; Sasaki, T. *J. Am. Chem. Soc.* **1983**, *105*, 2901-2902. (b) Tabushi, I.; Sasaki, T. *Tetrahedron Lett.* **1982**, *23*, 1913-1916.

(6) See also: (a) Jameson, G. B.; Molinalo, F. S.; Ibers, J. A.; Collman, J. P.; Brauman, J. I.; Rose, E.; Suslick, K. S. *J. Am. Chem. Soc.* **1980**, *102*, 3224-3237. (b) Collman, J. P.; Brauman, J. I.; Rose, El; Suslick, K. S. *Proc. Natl. Acad. Sci. U.S.A.* **1978**, *75*, 1052-1055. (c) Tsuchida, E.; Hasegawa, E.; Honda, K. *Biochem. Biophys. Acta* **1976**, *427*, 520-529.

(7) Interesting solid cooperativity is reported[6b] but further discussion is difficult considering the fact that the cooperativity coefficient is strongly dependent on the number of coupling sites. See ref 3.

(8) Fuhrhop, J.-H.; Smith, K. M. In "Porphyrins and Metalloporphyrins"; Smith, K. M., Ed.; Elsevier: New York, 1975; Chapter 19.

(9) (a) Collman, J. P.; Brauman, J. I.; Doxsee, K. M.; Halbert, T. R.; Bunnenberg, E.; Linder, R. E.; Lamar, G. N.; Gaudio, J. D.; Lang, G.; Spartalian, K. *J. Am. Chem. Soc.* **1980**, *102*, 4182-4192. (b) Hashimoto, T.; Dyer, R. L.; Crossley, M. J.; Baldwin, J. E.; Basolo, F. *J. Am. Chem. Soc.* **1982**, *104*, 2101-2109.

(10) Free gable shows some minor broadening, probably due to its slow tautomerism.

0002-7863/85/1507-4192$01.50/0

Scheme I

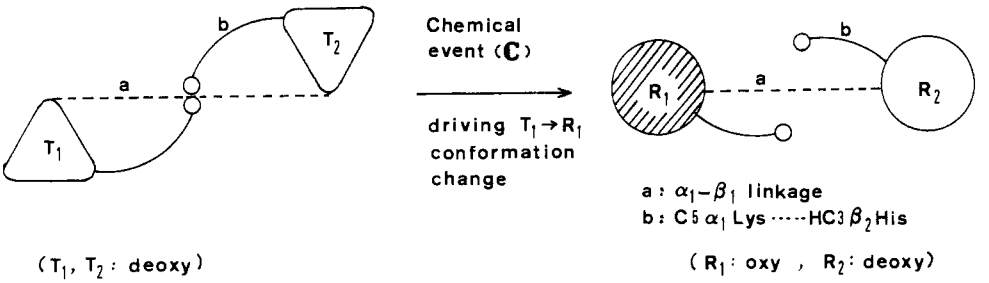

Table I. Base Binding Equilibria of Metal–Gable Porphyrin and Metal–TPP

porphyrin	metal M_1	metal M_2	log (binding constant)[a] DIM	1-MeIm	DPM	Pic
gable	Zn^{II}	Zn^{II}	7.5 ± 0.5	4.7 ± 0.1 (K_1)[f] 4.93 ± 0.04 (K_2)[f]	6.6 ± 0.3	4.13 ± 0.05 (K_1)[f] 4.20 ± 0.02 (K_2)[f]
	Zn^{II}	H_2			2.09 ± 0.12[e]	
	Co^{II}	Co^{II}	6.6 ± 0.2[b]	3.3 ± 0.1[b,q]	6.7 ± 0.2[b]	
	Fe^{II}	Fe^{II}	>6.6[c,i] 4.90 ± 0.01[c,g,j]	3.5 ± 0.5[c,g,i] 4.90 ± 0.02[c,g,j]		
	Fe^{II}	Fe^{II}	5.1 ± 0.1[d,h,k] 3.7 ± 0.1[d,g,h,l]			
TPP		Zn^{II}	4.67 ± 0.08	4.66 ± 0.08	4.17 ± 0.02	4.08 ± 0.02
		Co^{II}	3.48 ± 0.05[b]	3.4 ± 0.1[b]		3.11 ± 0.03[b]

[a] In benzene, 24 °C. [b] In DMF, −20 °C. [c] In benzene, 18 °C. [d] In DMF, 18 °C. [e] In DMF, 24 °C. [f] G{Zn(4),Zn(4)} + L ⇌ G{Zn(5)(L),Zn(4)} (K_1), G{Zn(5)(L),Zn(4)} + L ⇌ G{Zn(5)(L),Zn(5)(L)} (K_2). [g] Averaged value of the binding constants for two porphyrin moieties. [h] K_{DMF} = 16.9 ± 0.2 M^{-1} was obtained for DMF binding to the Fe^{II}_2·gable porphyrin in benzene. [i] 4 coordination ⇌ 5 coordination. [j] 5 coordination ⇌ 6 coordination. [k] 5′ coordination ⇌ 5# coordination. [l] 5# coordination ⇌ 6 coordination.

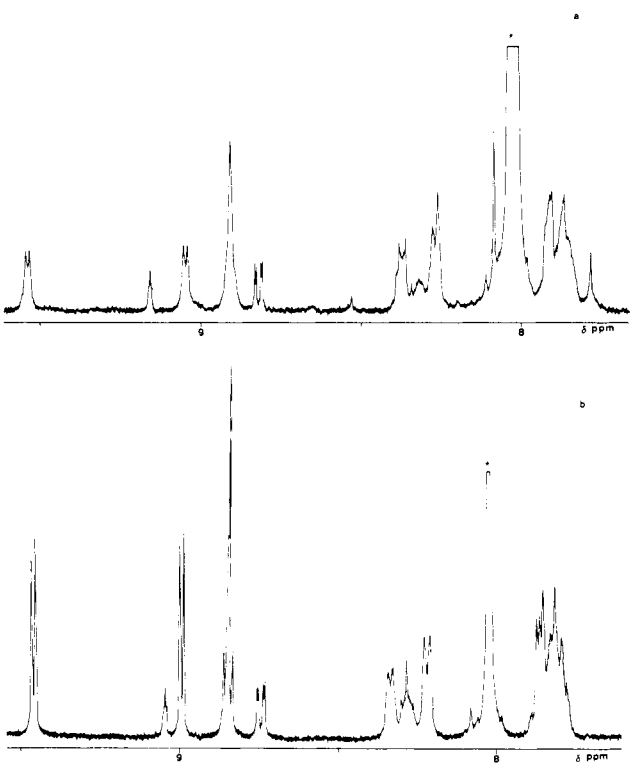

Figure 1. ^1H NMR spectra (400 MHz) of (a) gable porphyrin and (b) Zn_2·gable porphyrin in DMF-d_7. An asterisk indicates the solvent.

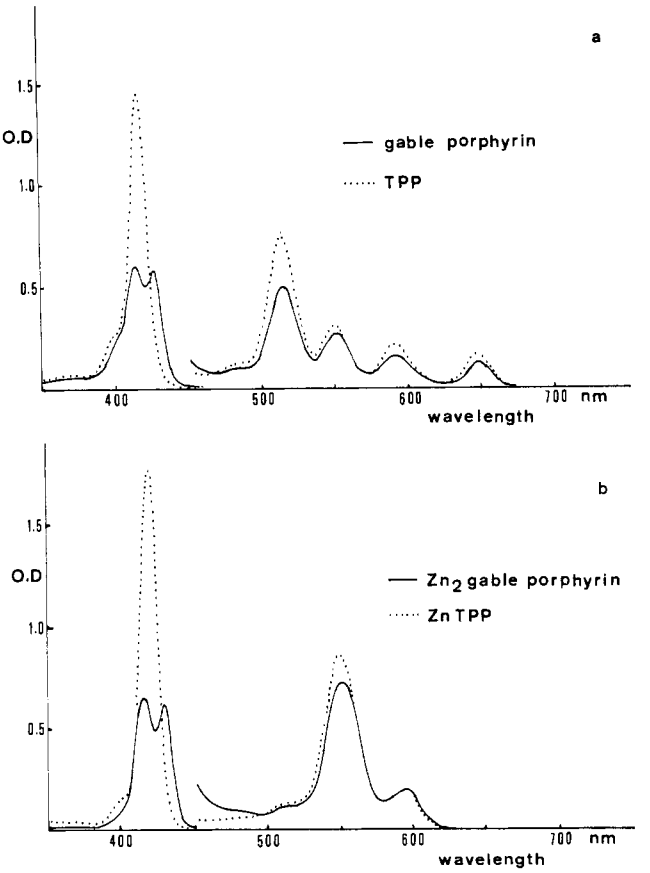

Figure 2. Electronic absorption spectra of (a) gable porphyrin and TPP and (b) Zn_2·gable porphyrin and ZnTPP in $CHCl_3$. The concentrations are 1.26 × 10^{-6} M (350–450 nm) and 1.47 × 10^{-5} M (450–750 nm) for gable porphyrin, 2.58 × 10^{-6} M (350–450 nm) and 3.23 × 10^{-5} M (450–750 nm) for TPP, 1.30 × 10^{-6} M (350–450 nm) and 2.01 × 10^{-5} M (450–750 nm) for Zn·gable porphyrin, and 2.60 × 10^{-6} M (350–450 nm) and 3.27 × 10^{-5} (450–750 nm) for ZnTPP.

porphyrins are unique, showing a sharp splitting in the Soret region (see Figure 2). The splitting seems to be correlated with weak interactions between the two porphyrins. The slight red shift from TPP (at 418 nm) to the center of the two separate absorptions of the free base gable porphyrin (416 and 428 nm in $CHCl_3$) is observed, again suggesting appreciable interaction between two porphyrin moieties. The splitting may be due to the nearly perpendicular orientation, since more strongly interacting face-to-face porphyrins[11] do not show any such Soret splittings.

Monomeric Ligand Coordination. The coordination of monomeric ligands to the bismetal–gable porphyrins was investigated

(11) (a) Collman, J. P.; Elliott, C. M.; Halbert, T. R.; Tovrog, B. S. *Proc. Natl. Acad. Sci. U.S.A.* **1977**, *74*, 18–22. (b) Collman, J. P.; Denisevich, P.; Konai, Y.; Marrocco, M.; Koval, C.; Anson, F. C. *J. Am. Chem. Soc.* **1980**, *102*, 6027–6036.

Chart I

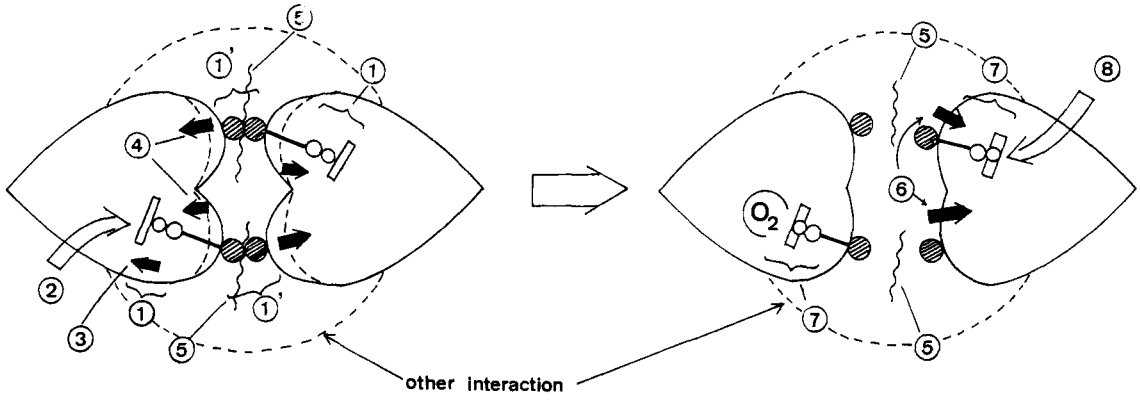

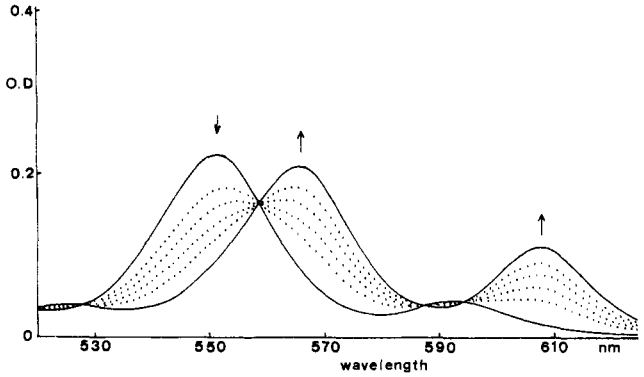

Figure 3. Electronic spectral changes occurring upon titration of a 4.80 × 10^{-6} M benzene solution of Zn_2·gable porphyrin with the following concentration of γ-picoline at 24 °C: 0, 3.38 × 10^{-5}, 6.76 × 10^{-5}, 1.35 × 10^{-4}, 2.70 × 10^{-4}, and 1.35 × 10^{-2} M.

by electronic spectroscopy (see Figure 3). The monomeric ligands used were 1-methylimidazole (1-MeIm) and γ-picoline (Pic). The coordination proceeds smoothly in benzene, leading to the corresponding base complexes. The association constants measured

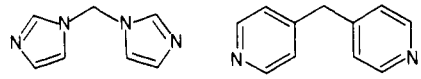

are listed in Table I. For coordination of monomeric ligands, the following two conclusions may be drawn.

(1) Basically, the base binding to gable porphyrin·M takes place normally. This is, the binding resembles the corresponding binding to TPP·M (e.g., with very similar association constants).

(2) Monomeric base binding to gable·M_2 proceeds in a clean, monophasic manner. That is, binding of the first base does not affect binding of the second base remarkably. This "normal" (*noncooperative*) binding is in a dramatic contrast to the *strongly cooperative* binding observed with the bridging ligands·gable·M^{II}_2 complex, which is discussed later.

Only for gable·Fe^{II}_2 does the formation of the hexacoordinate adduct compete with formation of the pentacoordinate species, but much less efficiently compared with simple Fe^{II}·porphyrin,[12] as discussed later.

Dimeric Bridging Ligand Coordination. Formation of Stable Allosteric Systems. Dimeric bridging ligands of appropriate sizes and shapes, DIM and DPM, were used for studying the binding behavior of gable·M_1 (monometal complex). In these cases,

(12) (a) Brault, D.; Rougee, M. *Biochem. Biophys. Res. Commun.* **1974**, *57*, 654–659. (b) Brault, D.; Rougee, M. *Biochemistry* **1974**, *13*, 4591–4597.

Scheme II

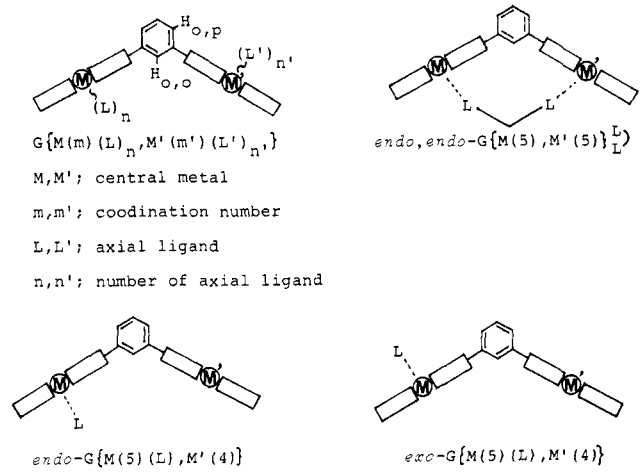

Scheme III. Association of M_2'Gable with Dimeric Bridging Ligands

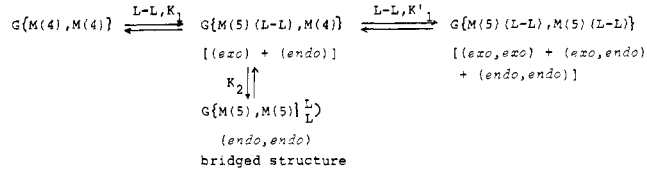

normal association contants, very similar to those for the TPP·M monomeric base systems, were observed (see Table I). Of the two stereochemically different binding sites for gable·Zn_1—exo and endo (see Scheme II)—the exo site demonstrated a greater preference. The exo stereoselectivity in binding was manifest in changes in the ^{1}H NMR chemical shifts of the central benzene proton of gable·M_1. As the base concentration increased, the resonance of $H_{o,p}$ located directly in the exo environment, experiences a small but appreciable upfield shift of ca. 0.01 ppm at 8.5 × 10^{-3} M (DPM) as observed by 400-MHz ^{1}H NMR. By contrast, the resonance of $H_{o,o}$, located in the endo environment does not.

When these bridging ligands coordinate to gable·M_2, they show a ligand concentration–complex formation profile (Figure 4) entirely different from the observed for binding to gable·M_1. The association constants for the formation of gable·M_2–bridging ligand complexes are much larger than those for the corresponding gable·M_1 complexes or gable·M_2–monomeric ligand complexes (see Table I). From the observed concentration dependence shown in Figure 4, K_2/K_1 in Scheme III is estimated to be much larger than unity.[13] In figure 4, calculated curves were obtained by a

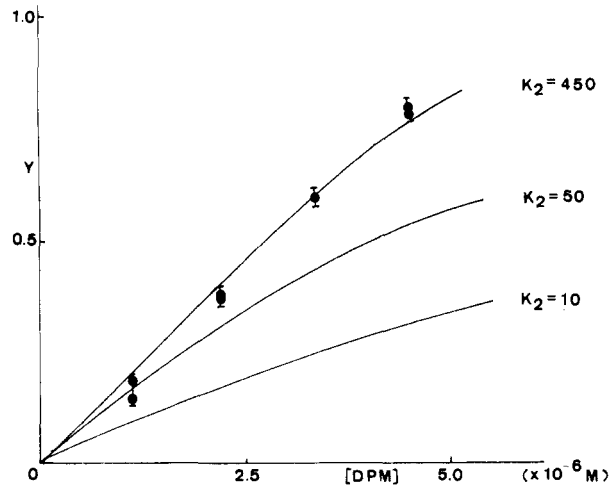

Figure 4. Estimation of the K_2 value for the Zn_2·gable·DPM system by a curve-fitting method. The concentration of Zn_2·gable porphyrin is 5.38 × 10^{-6} M in benzene; 24 °C; K_1 = 1.38 × 10^4 M^{-1} (see Scheme III); $Y = (A - A_0)/(A_0 - A_\infty)$. A_0 = absorbance at zero ligand concentration; A = absorbance at the designated ligand concentration; and A_∞ = saturated absorbance at high ligand concertration.

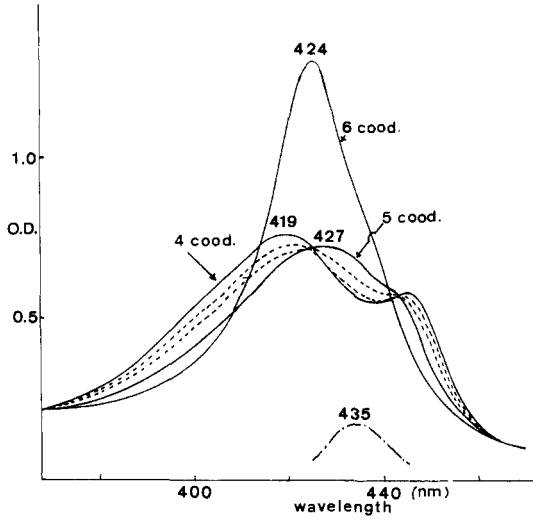

Figure 5. Electronic spectral changes occurring upon titration of a 5.0 × 10^{-6} M benzene solution of Fe^{II}_2·gable porphyrin with the following concentration of DIM at 18 °C: 0, 1.5 × 10^{-6}, 3.0 × 10^{-6}, 4.5 × 10^{-6}, and 6.4 × 10^{-4} M.

process of iterative arbitrary assumption until the best fit to the observed Y values was obtained. Calculation is based on Scheme III with the assumptions that (i) K_1 is equal to the corresponding TPP·M–bridging ligand association constant and (ii) K_1' is equal to K_1, giving the following values: K_2/K_1 = 450 M for DPM and 630 M for DIM. Therefore, dimeric bridging ligand·gable·M_2 complexes assume preferentially the bridged structure, over a wide range of ligand concentrations (e.g., for DPM 2 × 10^{-6} < [L–L] < 3 × 10^{-3} M, more than 90% of the complex is in the bridged structure), in spite of the fact that the endo side is considerably hindered than the exo side. Even for gable Fe^{II}_2, the pentacoordinate bridged state predominantes at low ligand concentration. A relatively good isosbestic point was obtained in certain

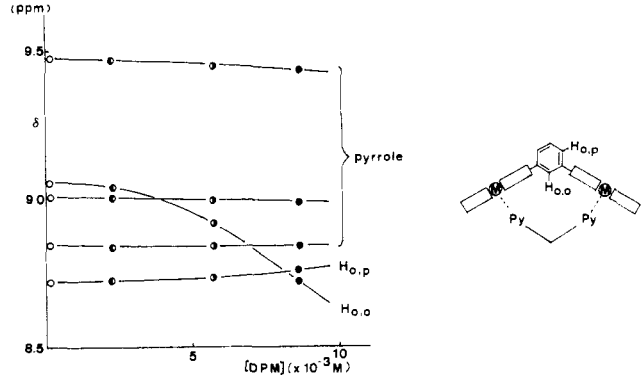

Figure 6. Dependence on DPM concentration of the chemical shifts of $H_{o,o}$ and $H_{o,p}$ of Zn·gable porphyrin in DMF-d_7: (○) [Zn_2·gable] = 3.56 × 10^{-3} M; (◐) [Zn_2·gable] = 3.31 × 10^{-3} M; (◑) [Zn_2·gable] = 2.90 × 10^{-3} M; (●) [Zn_2·gable] = 2.56 × 10^{-3} M.

Table II. Schemetic and Numeric Representation Description of Pseudoallosterism

major chemical interaction	pseudoallosteric system: proximity	allosteric system: different "chemical constraint"
molecular design, molecular mechanism	 L-L = DPM	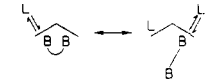 B-B = DPM; L = 1-MeIm
K_2/K_1	450/(1.3 × 10^4 × [DPM])	(38 ± 10)[DPM] = 1.56 × 10^{-4} M
Hill's coefficient	2.0	1.7 ± 0.1

Scheme IV

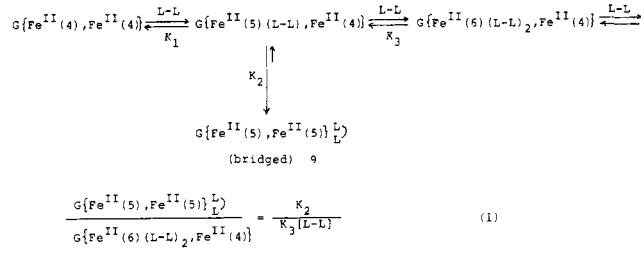

ligand concentrations in the ligand titration (Figure 5), demonstrating that the conversion of the tetracoordinate Fe^{II} to the *pentacoordinate* state is practically quantitative, where K_2/K_1 was estimated as 1300 M for DIM (see eq 1 of Scheme IV), based on the electronic spectrum ligand titration. The behavior is in sharp and interesting contrast to that for usual porphyrin·Fe^{II} complexes giving hexacoordination complexes predominantly.[12] The endo–endo bridged structure of the bridging ligand·gable·Zn_2 complexes has been well characterized by 400-MHz ^{1}H NMR. The absorption of $H_{o,o}$ (see Scheme II) affected by the endo topology (see Figure 6) experiences a remarkable upfield shift. The degree of this shift is entirely correlated with the bridging ligand concentration as shown in Figure 6. On the other hand, resonance of $H_{o,p}$ (exo) experiences only a tiny shift. Therefore, it is clearly demonstrated that gable porphyrin·biszinc and bis-iron(II) compelexes form the corresponding pentacoordinate bridging complexes with DIM or DPM as predominant, stable adducts in appropriate ligand concentration ranges. The formation of the endo,endo-gable–biszinc–bridging ligand complex does not concern an allosteric effect but concerns entropically favored bridging. To the resultant "allosteric" system, cooperative binding of a quest molecule is observed as discussed in the following section.

Cooperative Base Binding to the Artificial Allosteric System. The present observations that the bridged structure is much more favored than the open structure at appropriate base concentration provide an interesting possibility for the observation of artificial allosteric binding of a small "metallophilic" guest molecule.[4,5] Our

(13) (a) Jamson, G. B.; Molinaro, F. S.; Ibers, J. A.; Collman, J. P.; Brauman, J. I.; Rose, E.; Suslick, K. S. *J. Am. Chem. Soc.* **1980**, *102*, 3224–3237. (b) Jamson, G. B.; Molinaro, F. S.; Ibers, J. A.; Collman, J. P.; Brauman, J. I.; Rose, E.; Suslick, K. S. *J. Am. Chem. Soc.* **1978**, *100*, 6769–6770. (c) Cramor, S. P.; Eccles, T. K.; Kutzler, F.; Hodgson, K. O.; Doniach, S. *J. Am. Chem. Soc.* **1976**, *98*, 8059–8069. (d) Collman, J. P.; Bassolo, F.; Bunnenberg, E.; Collins, T. J.; Dawson, J. H.; Ellis, P. E., Jr.; Marrocco, M. L.; Moscowitz, A.; Sessler, J. L.; Szymanski, T. *J. Am. Chem. Soc.* **1981**, *103*, 5636–5648. (e) Kincaid, J.; Stein, P.; Spiro, T. G. *Proc. Natl. Acad. Sci. U.S.A.* **1979**, *76*, 549–552. Correction: *Ibid.* **1979**, *76*, 4156.

Table III. Experimental and Theoretical Parameters of Relative Cooperativity[a]

[B–B] (M)	K_{obsd} (M^{-1})	K_{calcd} (M^{-1})	n_{max}(obsd)	n_{max}(calcd)
6.24×10^{-6}	$K_1 = (3.2 \pm 0.4) \times 10^3$	$K_\alpha = 7.2 \times 10^3$	1.5 ± 0.1	1.53
	$K_2 = (3.0 \pm 0.3) \times 10^4$	$K_\beta = 7.8 \times 10^4$		
1.56×10^{-4}	$K_1 = 300 \pm 100$	$K_\alpha = 260$	1.7 ± 0.1	1.82
	$K_2 = (1.1 \pm 0.8) \times 10^4$	$K_\beta = 2.8 \times 10^4$		
1.04×10^{-3}	$K_1 = 110 \pm 20$	$K_\alpha = 190$	1.7 ± 0.1	1.70
	$K_2 = (3.7 \pm 0.8) \times 10^3$	$K_\beta = 5.9 \times 10^3$		
8.96×10^{-3}	$K_1 = 86 \pm 8$	$K_\alpha = 140$	1.4 ± 0.1	1.38
	$K_2 = 450 \pm 80$	$K_\beta = 600$		

[a] [Zn_2·gable] = 5.22×10^{-6} M; 24 °C inbenzene; B–B = DPM; L = 1-methylimidazole.

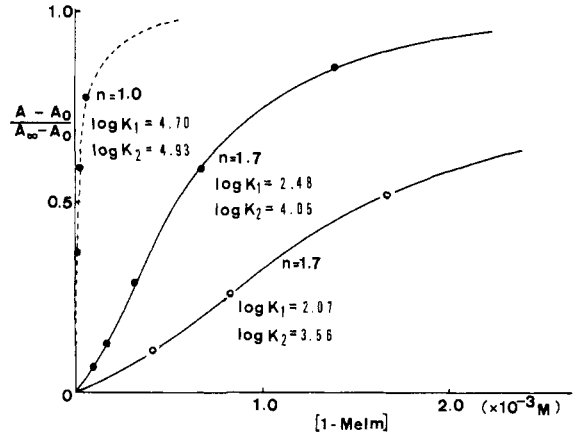

Figure 7. Cooperative 1-MeIm binding to the Zn_2·gable (DPM) complex (--●--) [DPM] = 0; (–●–) [DPM] = 1.56×10^{-4} M; (–○–) [DPM] = 1.04×10^{-3} M (Zn_2·gable] = 5.22×10^{-6} M in benzene; 24 °C. A_0 = absorbance at zero 1-MeIm concentration; A = absorbance at the designated 1-MeIm concentration; and A_∞ = saturated absorbance at high 1-MeIm concentration.

own definition of the artificial (generalized) allosteric system is already shown in Chart I and Scheme I. That the bridging complexes exist in the T structure is strongly suggested by electronic spectrum as discussed below. A bulky ligand such as 1,2-dimethylimidazole binds to a porphyrin·Fe^{II} to form the corresponding T-state pentacoordinate complex. The T structure is well established based on X-ray, XAFS, MCD, NMR, and Raman spectra.[13] We have measured the electronic spectrum of the pentacoordinate complex to find a small further blue shift from 1,2-dimethylimidazole to DIM, if difference spectrum is taken (see Table II). For hexacoordinate complexes, a similar clear blue shift from 429 nm for the $(1\text{-MeIm})_2$ complex to 424.5 nm for the DIM hexacoordinate complex is observed. These blue shifts are also observed for the corresponding CO complexes: TPP·Fe^{II}·1,2-Me_2Im·CO at 424, TPP·Fe^{II}·1-MeIm·CO at 427, gable·Fe^{II}_2·$(1\text{-MeIm})_2$·$(CO)_2$ at 429, gable·Fe^{II}_2·$(1,2\text{-Me}_2\text{Im})_2$·$(CO)_2$ at 422 nm, gable·Fe^{II}_2·DIM·$(CO)_2$ at 419. Therefore, it may be safely concluded that a bridging ligand (DPM or DIM) forms the pentacoordinate T-structure complex with gable·Fe^{II}_2.

The allosteric effect is clearly observed in the binding of 1-MeIm to the gable·Zn_2·DPM complex based on the electronic spectrum ligand titration as shown in Figure 7 and Table III. The observed magnitude of the cooperativity is sensitive to the bridging ligand concentration. At the optimal DPM concentration the Hill coefficient was estimated to be 1.7 from a plot of log $(Y/(1-Y))$ vs. log [1-MeIm].[15] A similar phenomena was observed in our O_2[5] and CO[14] cooperative binding systems. A most plausible mechanism to account for this concentration-dependent artificial allosteric effect is that shown in Scheme V. At the too low concentrations of the bridging ligand, the ligand binding to form the artificial allosteric system is not complete, leaving tetracoordinate sites, to which simple (noncooperative) 1-MeIm binding takes place. This leads to a decrease in the observed statistically

Scheme V

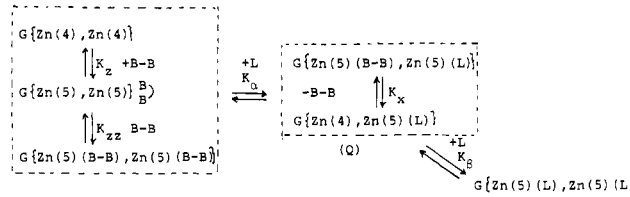

$$K_\alpha = \frac{K_w + K_w K_X [B\text{-}B]}{1 + K_Z [B\text{-}B] + K_Z K_{ZZ} [B\text{-}B]^2} \quad (2)$$

$$K_\beta = \frac{K_w}{1 + K_X [B\text{-}B]} \quad (3)$$

$$K_{app} = \frac{Q + R}{\{([G]_0 - Q - R) + Q\}[L]} = \frac{K_\alpha + K_\alpha K_\beta [L]}{1 + K_\alpha [L]} \quad (4)$$

$[L] \to 0 \quad K_{app} \to K_\alpha$

$[L] \to \infty \quad K_{app} \to K_\beta \qquad K_\beta > K_\alpha$ (positive cooperativity)

$[G]_0$: total concentration of Zn_2gable

[B-B] : concentration of bridging ligand

[L] : concentration of monodentate ligand

averaged cooperativity, while at too high concentrations of the bridging ligand population of the nonbridging R–R complexes increases (and "tension" or strain is relaxed) (see Scheme V), leading to a decrease in the observed statistically averaged cooperativity. Thus, at the moderate bridging ligand concentrations, observed cooperativity of the 1-MeIm binding becomes maximal. The populations of a variety of coordination complexes derived from gable·Zn^{II} and DPM are estimated based on the independently measured K values. This supports the proposed mechanism interpreting the observed cooperative base binding.

In conclusion, the most plausible molecular mechanism underlying the observed artificial allosteric effect in the monomeric base binding has been presented. This mechanism is in an excellent agreement with the mechanism presented previously for our cooperative O_2 binding system.[15]

Experimental Section

Instrument and Apparatus. Proton magnetic resonance spectra were recorded on either a JEOL PMX-60 continuous wave or a JEOL GX400 Pulse Foulier Transform NMR spectrometer. The chemical shifts are given in δ values from Me_4Si. Infrared spectra were obtained on a Hitachi 260-50 IR spectrometer. Electronic spectra were measured with a Union SM-401 high-sensitivity spectrometer and a Hitachi 340S spectrometer thermostated with a Thomas Scientific Model TRL-108 Circulation Type Handy Cooler. Melting points were measured with a Yanagimoto Micro Melting Point Apparatus and were corrected by use of pure benzoic acid (mp = 122.4 °C) as a standard. Mass spectra were obtained on a JEOL JMX-DX300 instrument. Elemental analysis were performed by the Microanalytical Laboratory at Kyoto University.

Thin-layer chromatography (TLC) was carried out on 0.25-mm E. Merck precoated silica gel plates (60F-254). For column chromatography, E. Merck silica gel 60 (70–230 mesh) was used. Preparation of ferrous porphyrins and subsequent manipulations requiring the exclusion of oxygen were carried out in a Vacuum Atmospheres Drybox, the internal atmosphere of which was constantly circulated through a diglyme

(14) Tabushi, I.; Sasaki, T.; unpublished results.
(15) Hill, A. V. *J. Physiol. London* **1910**, *40*, IV–VIII.

solution of $Mn^{II}TPP$ (1 g of $Mn^{III}TPPCl$ and 10 g of $NaBH_4$ in 200 mL diglyme) to remove traces of oxygen. Since all porphyrin samples were found to be light sensitive, handlings were performed in the dark as far as possible and all chromatography columns were wrapped in aluminum foil.

Materials. Commercially available chemicals were used directly as recieved unless otherwise noted. DMF was stirred for 12 h over powdered BaO (5 g/100 mL) at room temperature and fractionally distilled under reduced pressure just before use (a glass helix column (1 cm o.d. × 30 cm), reflux ratio 4:1, 16–17 °C (5 mmHg)). 1-MeIm and γ-picoline were distilled from KOH under Ar just before use. *N,N'*-Diimidazolylmethane (**2a**) was prepared according to the literature[15] and was recrystallized from a benzene–ethanol mixture:mp (benzene–ethanol) 173–174 °C (lit.[15] mp 171–172 °C); ν_{max} (KBr) 3200, 1500, 1480, 1380, 1340, 1270, 1220, 1090, 1080, 1050, 1020, 900, 890, 750 cm^{-1}; ^1H NMR ($CDCl_3$) δ 5.9 (s, 2 H), 6.5–7.1 (m, 4 H), 7.5 (br s, 1 H).

γ,γ'-Dipyridylmethane (2b). γ-Chloropyridine was prepared from 4-pyridylpyridine according to the literature.[16] γ,γ'-Dipyridylmethane (**2b**) was prepared by the reported procedure[17] with slight modifications (deoxygenation of liquid ammonia and EtMgBr treatment of the crude product). To 1 L of O_2-free, ligand ammonia (distilled twice under argon atmosphere) containing 8.5 g (0.15 mol) of KNH_2 was added 14 g (0.15 mol) of γ-picoline with stirring at −75 to −78 °C. After the mixture was stirred for 15 min, an ether solution containing 12.3 g (0.11 mol) of γ-chloropyridine was gradually added to it during 1 h under Ar atmosphere. Stirring was continued at the same temperature for a further 3 h. NH_4Cl (0.3 g) was then added and then ammonia allowed to evaporate under an Ar atmosphere. The residue so obtained was dissolved in H_2O (200 mL) and extracted with benzene (3 × 200 mL). The combined benzene extracts were dried over anhydrous Na_2SO_4. The Na_2SO_4 was filtered off and the benzene evaporated. The residue was distilled under reduced pressure to give 2.1 g (11%) of γ,γ'-dipyridylmethane (120–127 °C (1 mmHg)). γ,γ'-Dipyridylmethane (**2b**) thus distilled was further purified by treatment with EtMgBr in ether followed by distillation under reduced pressure. The moderately hygroscopic γ,γ'-dipyridylmethane was stored over KOH in a desiccator and redistilled under reduced pressure immediately before use. (**2b**): mp 36.5–37.5 °C; ν_{max} (KBr) 3020, 2900, 1950, 1600, 1560, 1500, 1410, 1220, 1070, 1000, 840, 800, 790, 750 cm^{-1}; ^1H NMR ($CDCl_3$) δ 3.78 (s, 2 H), 6.85 (m, 2 H), 8.23 (m, 2 H); MS, *m/e* (rel intensity) 171 (M^+ + 1, 14), 170 (M^+, 100), 169 (M^+ − 1, 23), 143 (2.2).

α,α,α'-Tribromo-*m*-xylene (3). In a 500-mL round-bottomed flask, fitted with a mechanical stirrer, a reflux condenser, a dropping funnel, and a gas inlet tube, was placed 104 g (0.98 mol) of *m*-xylene. The top of the reflux condenser was connected to a gas-absorption trap. A 500-W tungsten lamp was fixed 10 cm from the flask. N_2 gas was slowly bubbled into the flask. The stirrer was started, and the flask was irradiated by the lamp. When the xylene started boiling, 508 g (3.18 mol) of dry bromine (dried over P_2O_5 and distilled) was gradually added through the dropping funnel at a rate such that at any time there was only a small amount of unreacted bromine in the flask. Stirring and illumination were continued throughout the reaction, which required about 6 h. After all the bromine had reacted, the mixture was cooled and was left standing overnight. A small amount of crystalline α,α,-α',α'-tetrabromo-*m*-xylene was removed by decantation, and the brown liquid was used for the next preparation without further purifications (yield 319 g).

3-(Propionyloxymethyl)benzaldehyde (4). In a 1-L round-bottomed flask, fitted with a mechanical stirrer and a reflux condenser, was placed 460 mL of propionic acid. To the solution was added 63 g (1.5 mol) of NaOH pellets, and the mixture was stirred with cooling. After all the NaOH had dissolved, 100 g (0.29 mol) of crude α,α,α'-tribromo-*m*-xylene (**3**), obtained in the previous procedure, was added all at once. The mixture was heated under reflux for 6 h with stirring. Then, the mixture was cooled, and precipitates were filtered off. The dark brown filtrate was concentrated to about 150 mL under reduced pressure. To the resulting residue were added 300 mL of CH_2Cl_2 and 300 mL of saturated aqueous $NaHCO_3$ solution, and the mixture was stirred for 1 h. The lower layer was washed three times with 300 mL of saturated aqueous $NaHCO_3$ and 200 mL of H_2O and was dried over anhydrous Na_2SO_4. After the CH_2Cl_2 was distilled off, the residue was fractionally distilled under reduced pressure. The desired 3-(propionyloxymethyl)-benzaldehyde (**4**) boiled at 110–112 °C (1.3 mmHg). The yield was 44.5 g (23.6%). (**4**): ν_{max} (neat) 2900, 2730, 1740, 1690, 1610, 1590, 1460, 1380, 1340, 1180, 1080, 1030, 780, 690 cm^{-1}; ^1H NMR ($CDCl_3$) δ 1.2 (t, 3 H, *J* = 7.0 Hz), 2.4 (q, 2 H, *J* = 7.0 Hz), 5.15 (s, 2 H), 7.4–7.9 (m, 4 H), 9.9 (s, 1 H).

5,10,15-Triphenyl-20-(3'-propionyloxymethylphenyl)porphyrin (5). In a 2-L round-bottom flask fitted with a mechanical stirrer, a reflux condenser, and two dropping funnels were placed 1.5 L of propionic acid. The stirrer was started and the propionic acid was heated to reflux. From the dropping funnels 44.6 g of an aldehyde mixture (5.9 g (0.031 mol) of 3-(propionyloxymethyl)benzaldehyde (**4**) and 38.7 g (0.365 mol) of benzaldehyde) and 26.4 g (0.393 mol) of pyrrole were gradually added to the refluxing propionic acid over the course of 30 min. Stirring and heating were continued for another 30 min and, then, the propionic acid was distilled off under reduced pressure and the residue dissolved in 500 mL of $CHCl_3$. To the solution 200 mL of 10% aqueous Na_2CO_3 solution was added and the mixture was stirred for 30 min. The $CHCl_3$ layer was separated, washed with 10% aqueous Na_2CO_3 solution (2 × 200 mL), and dried over anhydrous Na_2SO_4. In order to remove polymeric by-products, 200 g of silica gel was added and the mixture shaken for 10 min. The silica gel was filtered off and washed well with $CHCl_3$. Both the filtrate and the washings were combined and evaporated to dryness. The residue was dissolved in 500 mL of benzene and applied to a silica gel column (8 cm o.d. × 50 cm). The column was eluted with benzene. The first fraction was concluded to consist of TPP (tetraphenylporphyrin) based on the following characteristic properties—TLC (silica gel, benzene) R_f = 0.91; λ_{max} ($CHCl_3$) 647, 591, 550, 514, 418 nm; ν_{max} (KBr) 1590, 1470, 1440, 1350, 1060, 960, 790, 690 cm^{-1}—which are identical with those of TPP independently prepared. The second band contained mainly the desired porphyrin ester (**5**) based on the following observations—TLC (silica gel, benzene) R_f = 0.48; λ_{max} ($CHCl_3$) 649, 592, 548, 513, 417.5 nm. Fractions showing these characteristic properties were collected and the solvent was distilled off. The residue was dried in vacuo to yield 4.1 g (19%) of **5**. The product, if necessary, was further purified by recrystallization from CH_2Cl_2–methanol. (**5**): mp (CH_2Cl_2–MeOH) 210–211 °C; ν_{max} (KBr) 2900, 1730, 1590, 1460, 1430, 1340, 1170, 1000, 960, 790, 690 cm^{-1}; ^1H NMR ($CDCl_3$) δ −2.67 (s, 2 H), 1.1 (t, 3 H, *J* = 7.0 Hz), 2.37 (q, 2 H, *J* = 7.0 Hz), 5.29 (s, 2 H), 7.4–7.8 (m, 11 H), 7.9–8.3 (m, 8 H), 8.70 (s, 8 H); FD-MS, *m/e* (rel intensity) 702 (14, M^+ + 2), 701 (33, M^+ + 1), 700 (100, M^+), 584 (20). Anal. Calcd for $C_{48}H_{36}N_4O_2 \cdot 0.5H_2O$: C, 81.20; H, 5.25. Found: C, 81.17; H, 5.20. λ_{max} ($CHCl_3$) 649, 592, 548, 513, 417.5 nm.

5-(3'-Hydroxymethylphenyl)-10,15,20-triphenylporphyrin (6). To a solution of 2.07 g (2.96×10^{-3} mol) of the porphyrin ester (**5**) in 100 mL of DMF placed in a 200-mL flask, 20 mL of aqueous NaOH (1.8 M) was added under N_2 atmosphere. The mixture was stirred for 2 h and poured into 400 mL of H_2O. The partially precipitated porphyrin was extracted into $CHCl_3$ (3 × 200 mL). The combined $CHCl_3$ extracts were washed with 10% aqueous K_2CO_3 (2 × 400 mL) and 300 mL of H_2O and dried over anhydrous Na_2SO_4. After the Na_2SO_4 was filtered off, the solution was concentrated to about 200 mL and applied to a column (silica gel, 5.5 cm o.d. × 30 cm). The column was eluted with $CHCl_3$ and fractions containing the hydroxymethylporphyrin (**6**) (checked by TLC; silica gel, CH_2Cl_2: R_f = 0.29 and IR spectrum: disappearance of the 1730-cm^{-1} absorption (C=O) observed in ester (**5**)) were collected. The combined fractions were concentrated to ca. 100 mL and then 100 mL of MeOH was added. From the solution dark purple crystals came out upon the slow evaporation of the solvent. The crystals which were collected were washed with MeOH (3 × 20 mL) and dried in vacuo. Yield 1.82 g (96%). (**6**): mp >300 °C; ν_{max} (KBr) 2900, 1590, 1460, 1430, 1340, 1000, 950, 790, 720, 690 cm^{-1}; ^1H NMR ($CDCl_3$) δ −2.72 (s, 2 H), 2.85 (s, 1 H), 4.85 (s, 2 H), 7.5–7.9 (m, 11 H), 8.0–8.3 (m, 8 H), 8.70 (s, 8 H); FD-MS, *m/e* (rel intensity) 646 (17, M^+ + 2), 645 (53, M^+ + 1), 644 (100, M^+); λ_{max} ($CHCl_3$) 648, 592, 549, 514, 418 nm.

5-(3'-Formylphenyl)-10,15,20-triphenylporphyrin (7). The formyl porphyrin (**7**) was prepared by two diffferent procedures.

Procedure I. All glass wares used in this procedure were soaked in aqua regia overnight, washed well with distilled water, and dried in vacuo. CH_2Cl_2 was distilled from $CaCl_2$ and redistilled from freshly prepared $Mn^{IV}TPP$ powder (ca. 100 mg/100 mL) to eliminate any reducing material present in CH_2Cl_2. Hexane was distilled from $CaCl_2$. $Mn^{IV}TPP$ was prepared according to the reported procedure:[18] In a 200-mL flask were placed 10 g (0.012 mol) of $Mn^{III}TPPCl$ and 30 mL of CH_2Cl_2. To a solution was added 5 mL of aqueous NaClO (active chlorine content: 2.5%), and the mixture was shaken vigorously for 10 min. During the procedure, the original green color changed to red-brown. Then, 150 mL of hexane was added to the mixture and the resulting precipitates of $Mn^{IV}TPP$ were filtered off and washed with hexane (2 × 20 mL). The solid $Mn^{IV}TPP$ obtained was used immediately for the following reaction without drying, since $Mn^{IV}TPP$ decomposes quickly even in purified CH_2Cl_2. To a solution of 0.3 g (4.6×10^{-4} mol) of the hydroxymethyl

(16) Schutze, W.; Schubert, H. *J. Pract. Chem.* **1959**, *8*, 306–313.
(17) Jerechel, D.; Fischer H.; Thomas, K. *Ber.* **1956**, *89*, 2921–2933.
(18) Jampolsky, L. M.; Kaiser, M. B. S.; Sternbach, L. H.; Goldberg, M. W. *J. Am. Chem. Soc.* **1952**, *74*, 5222–5224.

porphyrin (**6**) in 50 mL of CH_2Cl_2 placed in a 100-mL flask was gradually added small portions of the freshly prepared solid $Mn^{IV}TPP$ under N_2 atmosphere. Decrease of the hydroxymethyl porphyrin (**6**) was monitored by TLC (silica gel, CH_2Cl_2; R_f(aldehyde) = 0.75). The addition of $Mn^{IV}TPP$ was continued until the concentration of starting material decreased to about 10% of that initially used. The solution was concentrated to ca. 10 mL, and the resulting solution was loaded onto a column (silica gel, 2 cm o.d. × 15 cm). Elution with CH_2Cl_2 gave a trace amount of TPP as a first band and porphyrin aldehyde (**7**) as the second band. Fractions containing the porphyrin aldehyde were combined and concentrated to ca. 30 mL. MeOH (30 mL) was added to the concentrated solution and the solution was slowly evaporated at atmospheric pressure to give purple fine crystals which were then washed with MeOH (3 × 10 mL) and dried in vacuo to yield 0.26 g (87%) of **7**.

Procedure II. In a 500-mL, round-bottom flask were placed 2.0 g (3.1×10^{-4} mol) of the hydroxymethyl porphyrin (**6**) and 450 mL of CH_2Cl_2. After the hydroxymethyl porphyrin (**6**) dissolved completely, 10 g (0.115 mol) of active MnO_2[19] was added all at once. The mixture was stirred for 4 h at room temperature under Ar atmosphere. Any remaining MnO_2 powder was filtered off and washed with CH_2Cl_2 (5 × 50 mL). Filtrate and washings were combined and concentrated to ca. 200 mL. The solution was applied to a column (silica gel, 8 cm o.d. × 30 cm) and CH_2Cl_2 was used as an eluent. Appropriate fractions (checked by TLC silica gel, CH_2Cl_2; R_f = 0.75, IR (KBr) 1690 cm^{-1} (–CHO), and UV ($CHCl_3$) 646, 591, 551, 515, 418 nm) were collected and concentrated to ca. 100 mL, to which 100 mL of MeOH was added. The mixture was gradually concentrated to ca. 50 mL. On cooling in the refrigerator overnight, large amounts of fine purple crystals were deposited, which were collected by filtration, washed with MeOH (3 × 20 mL), and dried in vacuo. Yield 1.49 g (75 %) of (**7**): mp >300 °C; ν_{max} (KBr) 2900, 1690, 1590, 1460, 1340, 1250, 1210, 1180, 990, 960, 790, 720, 700, 690 cm^{-1}; ^1H NMR ($CDCl_3$) δ –2.80 (s, 2 H) 7.6–7.9 (m, 11 H), 8.0–8.4 (m, 8 H), 8.7–9.0 (m, 8 H), 10.35 (s, 1 H); ^{13}C NMR ($CDCl_3$) δ 117.8, 120.4, 120.6, 126.6, 127.4, 127.7, 128.6, 130.4, 131.2, 131.4, 134.5, 135.0, 135.1, 139.6, 142.0, 143.3, 146.6 (br), 192.3; FD-MS, *m/e* (rel intensity) 644 (22, $M^+ + 2$), 643 (67, $M^+ + 1$), 642 (100, M^+); λ_{max} ($CHCl_3$) 646, 591, 551, 515, 418 nm.

1,3-Bis(5′-(10′,15′,20′-triphenylporphinyl))benzene (1). In a 1-L, round-bottomed flask fitted with a mechanical stirrer and a reflux condenser was placed 850 mL of propionic acid. The stirrer was started and the propionic acid was heated to reflux. To the boiling propionic acid 7.84 g (0.0734 mol) of benzaldehyde, 1.49 g (0.00231 mol) of the porphyrin aldehyde (**7**), and 5.23 g (0.0781 mol) of pyrrole were added. The mixture was refluxed for 17 h with stirring and then the solvent was distilled off under reduced pressure. The residue was dissolved in 200 mL of CH_2Cl_2 and the solution was washed with 10% aqueous Na_2CO_3 (3 × 100 mL) to remove propionic acid. The CH_2Cl_2 layer was dried over anhydrous Na_2SO_4. Na_2SO_4 was filtered off and was washed with CH_2Cl_2 (3 × 50 mL). Filtrate and washings were combined and concentrated to ca. 150 mL. To the solution, 100 mL of hexane was slowly added with stirring and the mixture applied to a column (silica gel, 8 cm o.d. × 33.5 cm). The column was eluted with CH_2Cl–hexane (1:1) mixture. Appropriate fractions containing mainly gable porphyrin (**1**) (checked by TLC, silica gel, CH_2Cl_2–hexane (1:1); R_f = 0.71 and UV spectrum 416 and 428 nm (Soret)) were collected and evaporated to dryness. Crude gable porphyrin thus obtained was redissolved in 100 mL of CH_2Cl_2. To the solution of 50 mL of hexane was gradually added with stirring and applied to a second column (silica gel, 5.5 cm o.d. × 30.5 cm). The column was eluted with CH_2Cl_2–hexane (1:1) mixture. Appropriate fractions containing only gable porphyrin were collected. The combined fractions of gable porphyrin were evaporated to dryness. When the residue was kept for a while before use, it must be repurified by chromatography. Thus, the residue was redissolved in 100 mL of CH_2Cl_2 and passed through a short column (silica gel, 5 cm o.d. × 5 cm). A CH_2Cl_2 solution (100 mL) of the freshly prepared residue was concentrated to ca. 50 mL and 50 mL of MeOH was added. The mixture was slowly concentrated to ca. 30 mL, and the condensed solution was kept standing overnight in a refrigerator to give purple crystals which were isolated, washed with MeOH (3 × 10 mL), and dried in vacuo. Yield 0.588 g (22%). (**1**): mp >300 °C; ν_{max} (KBr) 1585, 1460, 1430, 1390, 1340, 1000, 960, 920, 798, 725, 695 cm^{-1}; ^1H NMR ($CDCl_3$) δ –2.60 (s, 4 H), 7.6–7.9 (m, 18 H), 8.0–8.4 (m, 13 H), 8.64 (d, 2 H), 9.12 (s, 1 H), 8.83 (s, 8 H), 8.98 and 9.30 (AB quartet, 8 H, J = 4.2 Hz); ^{13}C NMR ($CDCl_3$) δ 119.58, 120.27, 124.96, 126.65, 127.69, 131.12, 131.46, 133.80, 134.54, 140.13, 140.69, 142.21, 146.80 (br); λ_{max} ($CHCl_3$) 684, 592, 552, 515, 428, 416 nm.

Co^{II}_2·Gable (8a). In a 50-mL flask were placed 10 mg (8.3×10^{-6} mol) of gable porphyrin (**1**) and 30 mL of dry DMF (dried over CaH_2 and distilled under reduced pressure). The mixture was heated to reflux. When the gable porphyrin was dissolved, 60 mg (4.6×10^{-4} mol) of anhydrous $CoCl_2$ was added with stirring under Ar atmosphere. after 15 min, Co_2·gable began to precipitate. Metalation was complete after 1.5 h judging from the electronic spectrum of the solution (CH_2Cl_2 as solvent, gable porphyrin, 412, 425, 514, 548, 590, 645 nm; Co_2·gable, 412, 530 nm). The mixture was cooled to room temperature and 30 mL of H_2O was added. The precipitates formed were collected by suction filtration, washed with H_2O (5 mL) and MeOH (5 mL), and dried in vacuo. Crude product was dissolved in 50 mL of THF and applied to a column (silica gel, 3 cm o.d. × 40 cm). Elution with THF gave the fractions containing Co_2·gable, which were collected and evaporated to dryness. Yield 10 mg (91%). Co_2·gable was further purified by recrystallization from THF–hexane (1:1). (**8a**): mp >300 °C dec; ν_{max} (KBr) 2900, 1585, 1430, 1350, 1000, 920, 790, 750, 700 cm^{-1}; λ_{max} (DMF) 420, 534 nm.

Zn_1·Gable (8b). In a 100-mL, three-necked, round-bottomed flask fitted with a reflux condenser and an inlet for inert gas were placed 70 mL of methylene chloride and 101.1 mg (8.78×10^{-5} mol) of gable porphyrin. Methanol solution (30 mL) containing 19.0 mg (8.67×10^{-5} mol) of zinc acetate ($Zn(OAc)_2 \cdot 2H_2O$) was added slowly dropwise from a pasteur pipet into the refluxing methylene chloride solution over a period of 30 min with stirring (magnetic stirrer). To ensure that the reaction was complete, stirring and heating were continued for another 30 min. Production of monozinc–gable was checked by TLC (alumina, CH_2Cl_2–hexane) (2:1), R_f(Zn_2·gable) = 0.10, R_f(Zn_1·gable) = 0.49, R_f(gable) = 0.90). The reaction mixture was then evaporated to dryness. Methylene chloride (80 mL) was added to dissolve almost all of the solid and then 40 mL of hexane was added to the solution. The mixture was then loaded onto a neutral alumina column (5.5 cm o.d. × 30 cm, 550 g) and eluted with methylene chloride/hexane (2:1). This eluted the free base gable porphyrin. The amount of methylene chloride was then gradually increased, causing monozinc–gable to be eluted. Finally, only methylene chloride was used as an eluent, eluting dizinc–gable from the column. The purity of each fraction was checked by TLC on neutral alumina with methylene chloride/hexane (2:1) as an eluent. Yield was 42.4 mg (41.8%). (**8b**): mp >300 °C; ν_{max} (KBr) 1600, 1442, 1388, 1075, 1005, 964, 923, 802, 712, 702 cm^{-1}; ^1H NMR (DMF-d_7) δ –2.7 (s, 2 H), 7.7–7.9 (m, 18 H), 8.2–8.4 (m, 13 H), 8.78 (dd, J_1 = 7.70 Hz, J_2 = 1.84 Hz, 2 H), 8.86 (AB quartet, J = 1.83 Hz, 4 H), 8.91 (br s, 4 H), 9.00 (d, J = 4.58 Hz, 2 H), 9.05 (d, J = 5.13 Hz, 2 H), 9.11 (br s, 1 H), 9.47 (d, J = 4.58 Hz, 2 H), 9.54 (d, J = 4.39 Hz, 2 H); 2 H); FD-MS *m/e* (rel intensity) 1217 (25), 1216 (25), 1215 (100), 1214 (48), 1213 (37, M^+); λ_{max} ($CHCl_3$) 647, 593, 551, 515, 429, 415 nm.

Zn^{II}_2·Gable (8c). To a solution of 82 mg (7.1×10^{-5} mol) of gable porphyrin (**1**) in 20 mL of $CHCl_3$ in a 50-mL flask was added 100 mg of $Zn(OAc)_2 \cdot 2H_2O$ dissolved in 5 mL of MeOH. The mixture was refluxed for 20 min with stirring, and 20 mL of H_2O was added. The lower layer was separated, washed with H_2O (2 × 20 mL), and dried over Na_2SO_4. The Na_2SO_4 was filtered off and washed with $CHCl_3$ (3 × 10 mL). Filtrate and washings were combined and evaporated to dryness. To the residue, 200 mL of benzene was added and heated with stirring until all the solid had dissolved. This hot benzene solution of zinc complex was applied to column (silica gel, 8 cm o.d. × 17 cm). Elution with benzene gave Zn^{II}_2·gable as the first band (checked by TLC, silica gel, benzene, R_f = 0.68 and with UV spectrum; 416 and 431 nm (Soret band in $CHCl_3$)). Appropriate fractions were combined and evaporated to dryness to yield 82 mg (90%) of **8c**. Zn^{II}_2·gable can be further purified by recrystallization from toluene. (**8c**): mp >300 °C; ν_{max} (KBr) 1595, 1440, 1340, 1000, 990, 925, 790, 750, 710, 610 cm^{-1}; ^1H NMR ($CDCl_3$–Me_2SO-d_6 = 4:1) δ 7.6–7.8 (m, 18 H), 8.1–8.3 (m, 13 H), 8.04 (d, 2 H, J = 7.7 Hz), 8.82 (s, 8 H), 8.98 (d, 4 H, J = 4.6 Hz), 9.02 (s, 1 H), 9.34 (d, 4 H, 4.6 Hz); λ_{max} ($CHCl_3$) 594, 552, 431, 416 nm.

Fe^{III}_2·Gable Cl_2 (8d). In a 300-mL, round-bottomed flask were placed 101 mg (0.088 mmol) of gable porphyrin (**1**), 315 mg (2.48 mmol) of anhydrous $FeCl_2$, and 200 mL of dry DMF (dried over CaH_2 and distilled under reduced pressure). The mixture was heated to reflux under an argon atmosphere. The reaction was followed by monitoring changes in the electronic spectrum (solvent CH_2Cl_2–trace HCl, λ_{max} (H_4^{4+}·gable) 449 nm, λ_{max} (Fe^{III}_2·gable) 417 nm). The reaction was complete after 1 h. The solvent was removed under reduced pressure and then 100 mL of CH_2Cl_2 was added to the residue. The CH_2Cl_2 solution was washed with H_2O (3 × 100 mL) and 3 drops of concentrated HCl was added to decompose the μ-oxo compound. The CH_2Cl_2 solution was dried over anhydrous Na_2SO_4. Na_2SO_4 was filtered off and washed with CH_2Cl_2

(19) Tabushi, I.; Koga, N. *Tetrahedron Lett.* **1978**, 5017–5020.
(20) Attenburrow, J.; Cameron, A. F. B.; Chapman, J. H.; Evans, R. M.; Hems, B. A.; Jenson, A. B. A.; Walker, T. *J. Chem. Soc.* **1952**, 1094–1111.
(21) Collman, J. P.; Bassolo, F.; Bunnenberg, E.; Collins, T. J.; Dawson, J. H.; Ellis, P. E., Jr.; Marrocco, M. L.; Moscowitz, A.; Sessler, J. L.; Szymanski, T. *J. Am. Chem. Soc.* **1981**, *103*, 5636–5648.

(3 × 20 mL). Filtrate and washings were combined and concentrated to ca. 20 mL and then applied to a silica gel column (3 cm o.d. × 33 cm). The elution of Fe_2·gable Cl_2 with CH_2Cl–MeOH (15:1) was followed by TLC (silica gel, R_f = 0.3 [CH_2Cl_2–MeOH = 15:1); UV λ_{max} (benzene) 689, 622, 572, 507, 420 nm): All fractions containing Fe_2·gable Cl_2 were combined and concentrated to 30 mL. Hexane (30 mL) was added and the mixture was slowly condensed to 20 mL and kept standing overnight in a refrigerator. Fine dark-purple crystals formed were filtered, washed with hexane (3 × 3 mL), and dried in vacuo to yield 96 mg (0.072 mmol, 82.1%) of **8d**. Fe_2·gable Cl_2 was further purified by recrystallization from toluene. (**8d**): mp >300 °C dec; ν_{max} (KBr) 2950, 2800, 1600, 1480, 1440, 1340, 1260, 1080, 1000, 900, 800, 760, 720, 700, 440, 360 cm^{-1}; FD-MS, *m/e* (rel intensity) 1331 (53, M^+ + 3), 1330 (91, M^+ + 2), 1329 (100, M^+ + 1), 1328 (23, M^+), 1327 (56, M^+ – 1), 1294 (72, M^+ – Cl + 1), 1259 (13, M^+ – 2Cl + 1); λ_{max} (benzene) 689, 622, 572, 507, 420 nm.

Fe^{II}_2·Gable (8e). All manipulations were performed in the drybox (filled with oxygen-free argon) to avoid any oxidation of Fe^{II}·porphyrin. A mixture of 2.0 mg (1.6 × 10^{-6} mol) of Fe^{III}_2·gable Cl_2 (**8d**) in 5 mL of benzene and 0.5 mL of aqueous buffer solution (0.1 M phosphate, pH 6.86) was deoxygenated by 3 freeze–pump–thaw cycles (2 × 10^{-6} torr). To the mixture 20 mg (1.1 × 10^{-4} mol) of solid $Na_2S_2O_4$ was added and the mixture was stirred vigorously for 30 min. The resulting orange-red solution of crude bisferrous gable porphyrin (**8e**) was dried over anhydrous Na_2SO_4 and applied to a specially prepared alumina column (vide infra). The column was eluted with oxygen-free methanol (1%) in benzene to afford the fractions containing **8e** alone. The fractions were combined and evaporated to dryness to give pure **8e**: λ_{max} (benzene) 420, 446, 539 nm. The electronic spectrum of **8e** indicates no contamination with oxy-, μ-oxo dimer or other impurities.

Preparation of the Alumina Column. A suspension of 4 g of neutral alumina (Wolem activity I) and 0.15 g of $Na_2S_2O_4$ in 20 mL of deoxygenated H_2O was stirred for 30 min under Ar atmosphere. Alumina was collected by decantation, washed with deoxygenated H_2O (6 × 10 mL), and dried in vacuo (1 × 10^{-3} torr, at room temperature) for 12 h. The pretreated alumina was placed into a column and used for the purifications of bisferrous gable porphyrin. To remove trace oxygen adsorbed on alumina, 1 mL (ca. 1 × 10^{-4} M) of benzene solution of bisferrous gable porphyrin was passed through the column by use of benzene–methanol (100:1) as an eluent just before use.

Measurement of Base Binding Equilibria. Because of the extreme oxygen sensitivity of ferrous porphyrins in solution, the 4-coordinate (baseless) ferrous porphyrins were freshly prepared in the drybox just before use. In a typical experiment, 2.0 mg of Fe^{III}_2·gable Cl_2 was dissolved in benzene (5 mL) and 0.5 mL of buffer (0.1 M phosphate, pH 6.86) was added. The mixture was deoxygenated by freeze–pump–thaw cycles (three times, 2 × 10^{-6} torr), and 20 mg of solid $Na_2S_2O_4$ was added under Ar. After vigorous shaking for 30 min, the brown solution turned to an orange-red. The benzene layer was removed by pasteur pipet in the drybox filled with oxygen-free argon and dried over anhydrous Na_2SO_4. Ferrous gable porphyrin was purified through a special column pretreated with a reducing reagent (vide supra). λ_{max} (benzene) 420, 445, 534 nm. Equilibrium constants were determined by visible spectrophotometric titration. To a benzene solution (2.0 mL) of the bisferrous gable porphyrin was added 0.05–0.4 mL of the benzene solution of the axial ligand, and the total volume of each mixture was then adjusted to 2.5 mL by the addition of deoxygenated benzene. Then, the spectra were recorded at 18 °C in the 350–750 nm range.

Equilibrium constants for the base binding reaction of Co^{II}_2·gable and Zn^{II}_2·gable were similarly measured by a spectrophotometric titration method. Aliquots of a solution containing an appropriate amount of an axial ligand were added to a 1-mL solution of Co^{II}_2·gable or Zn^{II}_2·gable and the total volume was adjusted to 5 mL under an Ar atmosphere. The spectra were recorded at 18 °C in the 750–350 nm region.

Registry No. 8a, 85318-78-1; **8b**, 96481-87-7; **8c**, 96481-88-8; **8d**, 96502-29-3; **8e**, 96481-89-9; ZnTPP, 14074-80-7; CoTPP, 14172-90-8; DIM, 84661-56-3; 1-MeIm, 616-47-7; DPM, 60776-05-8; Pic, 108-89-4.

Synthesis and Characterization of Phenolate-Bridged Copper Dimers with a Cu–Cu Separation of >3.5 Å. Models for the Active Site of Oxidized Hemocyanin Derivatives

Thomas N. Sorrell,*[1a] Charles J. O'Connor,[1b] Oren P. Anderson,[1c] and Joseph H. Reibenspies[1c]

Contribution from the Departments of Chemistry, The University of North Carolina at Chapel Hill, Chapel Hill, North Carolina 27514, the University of New Orleans, New Orleans, Louisiana 70148, and Colorado State University, Fort Collins, Colorado 80523. *Received June 11, 1984*

Abstract: Described are the synthesis and characterization of the new binucleating ligand 2,6-bis(bis[2-(1-pyrazolyl)-ethyl]amino]-*p*-cresol (Hbpeac) and two of its copper(II) derivatives. The ligand provides four donors, including a bridging phenoxide, to each metal ion. An "exogenous" ligand completes the coordination sphere of each copper. Both the μ-acetato (**1a**) and the μ-1,3-azido (**1b**) copper(II) complexes have been characterized by X-ray crystallography. In both structures, the coordination spheres of the copper(II) ions are distorted from a square-pyramidal geometry toward a trigonal-bipyramidal arrangement. The distortion is more pronounced in the acetato complex and accounts for the difference between the two compounds in terms of their magnetic behavior. Variable temperature magnetic susceptibility measurements demonstrate strong antiferromagnetic coupling ($2J = -1800$ cm^{-1}) for the azido derivative but negligable magnetic interaction between the copper ions in the acetato complex. The magnetic behavior, electronic spectrum, and structure of the azide derivative suggest that this complex is an excellent structural model for the oxidized azide derivative of hemocyanin. Crystal data for $C_{32}H_{42}Cl_2Cu_2N_{10}O_{12}$ (**1a**) are as follows: orthorhombic, a = 13.999 (5) Å, b = 23.046 (9) Å, c = 12.523 (5) Å, V = 4043 Å^3, Z = 4, space group = $P2_12_12_1$. Crystal data for $C_{31}H_{41}Cl_2Cu_2N_{13}O_{13}$ (**1b**) are as follows: orthorhombic, a = 12.977 (2) Å, b = 13.188 (3) Å, c = 22.033 (6) Å, V = 3771 Å^3, Z = 4, space group = $P2_12_12_1$.

Hemocyanin (Hc)[2] is a copper-containing protein which functions to transport dioxygen in the hemolymph of several species of arthropods and mollusks. Its binuclear active site has been extensively characterized spectroscopically,[3,4] and its reactions have been used to generate many interesting inorganic species which until recently have had (or in some cases still have) no counterparts among synthetic complexes.[5]

(1) (a) University of North Carolina. (b) University of New Orleans. (c) Colorado State University.

(2) Abbreviations used in this paper: Hc, hemocyanin; HcO_2, oxyhemocyanin; bpeac, the anion of 2,6-bis(bis[2-(1-pyrazoyl)ethyl]amino)-*p*-cresol; DMF, dimethylformamide; OAc, acetate; THF, tetrahydrofuran.

(3) (a) Solomon, E. I. In "Copper Proteins"; Spiro, T. G., Ed.; Wiley: New York, 1981; Chapter 1. (b) Solomon, E. I.; Penfield, K. W.; Wilcox, D. E. *Struct. Bonding (Berlin)* **1983**, *53*, 1–57.

(4) (a) Woolery, G. L.; Powers, L.; Winkler, M.; Solomon, E. I.; Spiro, T. G. *J. Am. Chem. Soc.* **1984**, *106*, 86–92. (b) Wilcox, D. E.; Long, J. R.; Solomon, E. I. *Ibid.* **1984**, *106*, 2186–2194.

0002-7863/85/1507-4199$01.50/0